Chapter 1

NO formation and destruction in laminar premixed hydrocarbon flames

This chapter provides background information on NO formation, and flue-gas recirculation and burner stabilization as NO emission control strategies in one-dimensional laminar premixed methane-air flames

1.1 Chemistry and physics of flat laminar premixed methane-air flames

1.1.1 Flat laminar premixed flames

Flat laminar premixed flames are the workhorse of many combustion laboratories, since the one-dimensional character of these steady flames offers great advantages for modeling, and allow a straightforward comparison with experiments.

In a flat laminar premixed flame, fuel and oxidizer (for example methane and air) are fully mixed prior to combustion. The premixed gas composition is usually expressed in terms of the equivalence ratio (ϕ), which is defined as the molar ratio of fuel and oxidizer with respect to that at stoichiometric conditions. A premixed flame is considered stoichiometric if oxidizer and fuel are in the ratio prescribed by the balanced chemical equation for combustion, for example:

$$CH_4 + 2O_2 \rightarrow CO_2 + 2H_2O \qquad \text{(R 1.1)}$$

Conditions of excess fuel (ϕ>1) or deficiency of fuel (ϕ<1) are referred to as fuel-rich or fuel-lean, respectively.

The coupling of heat and mass transport and chemical reaction leads to a spatial structure, the flame, which determines the path from reactants to products. The structure of a flat laminar-premixed flame is schematically shown in Figure 1.1:

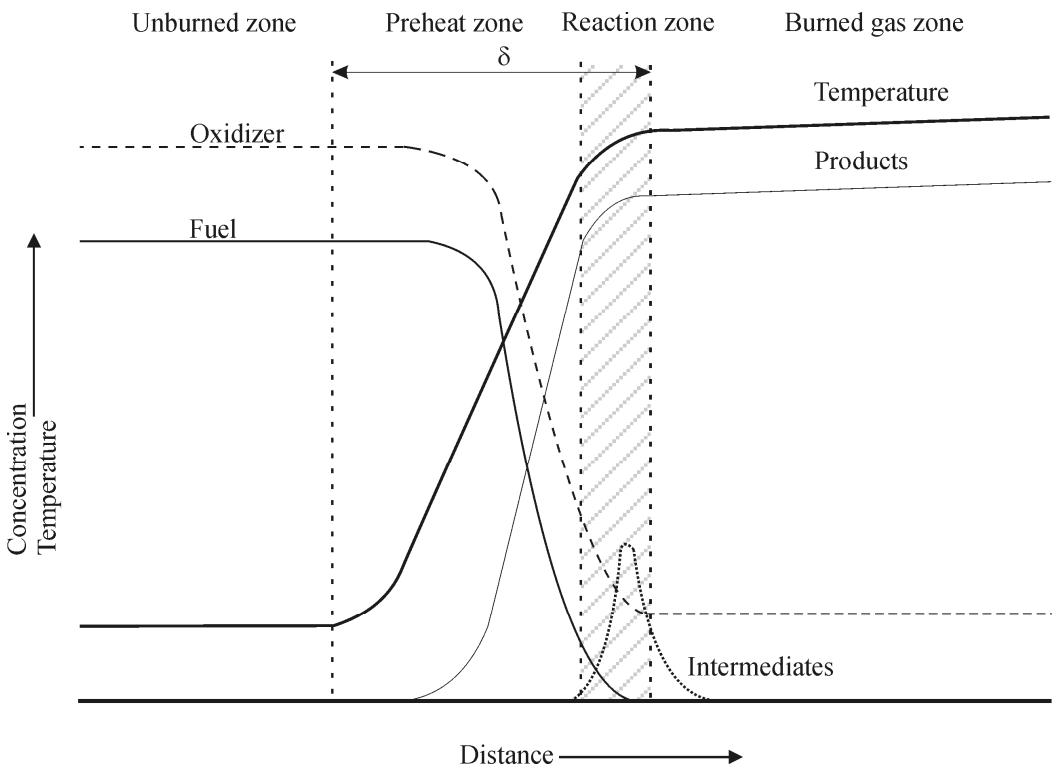

Figure 1. 1. Schematic representation of premixed flame structure.

Premixed flame structure can be divided into four zones: unburned zone, preheat zone, reaction zone and burned gas zone. The unburned mixture of fuel and oxidizer is delivered to the preheat zone at ambient conditions, where the mixture is warmed by upstream heat transfer from the reaction zone. In the reaction zone, the fuel is rapidly consumed and the bulk of chemical energy is released. The thickness of the flame front (δ, see Figure 1.1) is ~ 0.5 mm at atmospheric pressure and ~ 5 mm at 25 Torr, depending not only on pressure but also on initial temperature and equivalence ratio [1-3]. This thin flame front implies steep species and temperature gradients, which provide the driving forces for the flame to be self-sustaining. In the reaction zone, temperature is high enough for creating a large radical pool. Finally, in the burned zone, radicals recombine, and both temperature and major species concentrations approach their equilibrium values. However, the concentrations of minor species in this region can deviate substantially from their equilibrium values.

The velocity with which a flat flame front propagates with respect to the unburned fuel/oxidizer mixture is called the laminar burning velocity, S_L, and is strongly dependent upon fuel and oxidizer type, equivalence ratio and

temperature of unburned fuel/oxidizer mixture. In the laboratory frame, where the unburned fuel/oxidizer mixture propagates with velocity v, the speed of the flame front v_{fr} is $v\text{-}S_L$. In practice, one-dimensional flames are created by supplying the fuel/oxidizer mixture through porous material, effectively creating a uniform flow field, which is schematically illustrated in Figure 1.2:

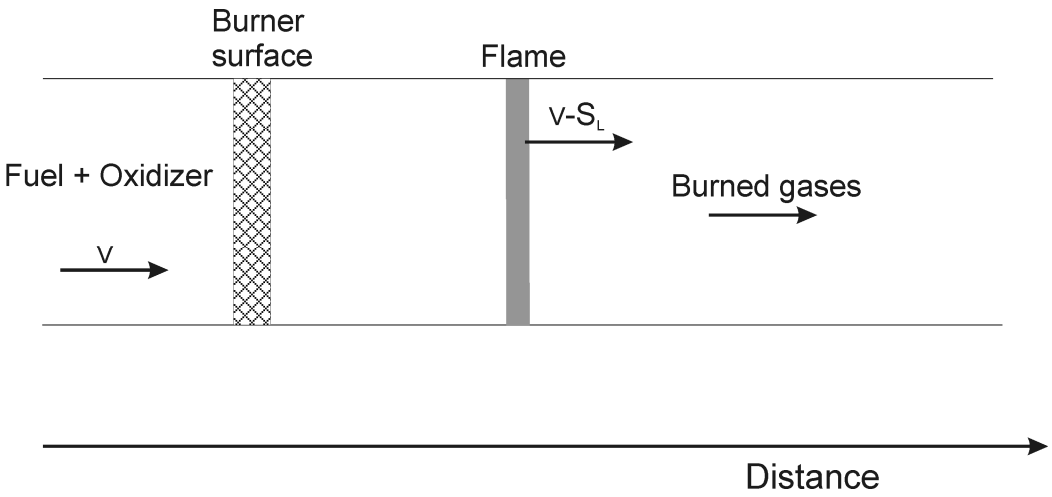

Figure 1. 2 Schematic illustration of flame burning downstream of a porous burner, where v is unburned gas velocity, S_L is laminar burning velocity.

Since the laboratory frame is attached to the burner, three possible idealized situations may occur, depending on the relation between v and S_L. First, if $v>S_L$ the flame will move away from the burner, i.e., the flame will blow off. If $v=S_L$, the flame will keep its position relative to the burner surface, and be "aerodynamically stabilized". In this case, neglecting possible radiative losses from the flame to the surroundings, the enthalpy in the fuel is solely manifest in the temperature of the burned gases, and the flame is referred to as an "adiabatic" or "free" flame. The temperature corresponding to an adiabatic flame is the maximum flame temperature that can be achieved for a given fuel-oxidizer composition. If $v<S_L$, the flame will move towards the burner and will attempt to enter the burner. Since the pores of the idealized burner are assumed to prevent the flame from entering the burner, the flame will transfer heat to the burner to lower the actual burning velocity to the flow velocity; in this condition the flame is referred to be as being 'stabilized' by the burner surface. Later in this chapter we will discuss burner stabilization in more detail.

1.1.2 Conservation equations for an one-dimensional steady laminar premixed flame

In a one-dimensional steady flame at constant pressure, the effects of viscosity, radiation and gravitation are generally neglected [3,4]. In this case, the governing equations can be written as shown below [4].

Overall conservation of mass

The conservation of total mass states:

$$\frac{d}{dx}(\rho v) = 0, \qquad (1.1)$$

where ρ is the overall mass density and v is the mean mass velocity. From equation (1.1) follows that the product of the density and the velocity, the mass flux, is constant and independent of x.

Conservation of mass of a particular species *i*

$$\frac{d}{dx}[y_i \rho (v + V_i)] = R_i, \qquad \text{(i=1…K)} \qquad (1.2)$$

where y_i is the species mass fraction and V_i is the species diffusion velocity, expressing the molecular transport caused by concentration gradients of species *i*. When the concentration of i^{th} component is low, Flick's law [3] can be used to calculate V_i. An important property is that the system of equations (1.1) and (1.2), contains K linearly independent equations. Because the chemical reaction does not change the element composition, the total mass production rate $\sum R_i = 0$. Therefore summation of equation (1.2) over K yields equation (1.1).

In flames, the time scales of transport processes, such as diffusion and heat conduction are comparable to the time scales of chemical reactions. Therefore, determining combustion properties requires information on the rates of both transport processes and chemical reactions.

Equation of state

The equation of state is given by:

$$p = RT\sum_i \frac{y_i \rho}{M_i}, \tag{1.3}$$

where p is the pressure, R the universal gas constant, T the temperature and M_i the molar mass of species i. Assuming that the dependence of the diffusion velocity V_i on the temperature and species concentrations is known, the above-described system consists of (K+1) linearly independent equations and contains (K+2) unknown parameters: y_i, v, ρ and T. Thus, the system contains more unknown parameters than equations and a solution is only possible if one of the parameters is specified, or if an extra equation is added to the system, such as the equation for the conservation of energy.

Conservation of energy

The conservation of energy is expressed as:

$$\frac{d}{dx}\left[\sum_i y_i \rho H_i \left(v + V_i\right) - \lambda \frac{dT}{dx}\right] = 0, \tag{1.4}$$

where H_i is the specific enthalpy of the ith species and λ the thermal conductivity of the mixture. The conservation of energy states that the sum of energy transport by means of convection (first term), diffusion (second term) and conduction (third term) must be equal to zero.

Although with the addition of this equation the system of equations can now be solved, for burner-stabilized flames one often chooses to use measured temperature profiles as input to the model. This is intended to "correct" the model predictions for differences in chemistry that any discrepancies in the temperature profile may cause.

Several software packages have been developed to solve the set of governing equations described above. In this work, the PREMIX code of the

CHEMKIN II package [5] is used. This software package can be used to calculate both burner-stabilized and free flames.

1.1.3 Chemical production rate, R_i

The combustion process of methane and oxygen is not a simple single-step reaction as equation (R 1.1) may suggest, but takes place in many steps, in which several hundred elementary reactions occur among several tens of chemical species. Thus, not only H_2O and CO_2 are formed in the process, but also species such as NO, CO, NO_2, OH, CH and others are formed by means of complex chemical mechanisms. The equation for conservation (1.2) needs to be solved for each species that participates in the process.

If N species are considered, every chemical reaction j can be presented as:

$$\sum_{i=1}^{N} r_{ij} A_i \underset{k_{fj}}{\overset{k_{rj}}{\leftrightarrows}} \sum_{i=1}^{N} p_{ij} A_i \,, \tag{1.5}$$

where A_i represents the ith component, r_{ij} and p_{ij} are stoichiometric coefficients of reactants and products respectively. Suppose we are only interested in the rate of change of species A_i, in this case the following expression can be found based on equation (1.5):

$$\frac{d[A_i]}{dt} = -k_{fj} r_{ij} \prod_{i=1}^{N} [A_i]^{r_{ij}} + k_{rj} p_{ij} \prod_{i=1}^{N} [A_i]^{p_{ij}} \tag{1.6}$$

where [] denote the molar concentration of species A_i. The reaction rate constant is often expressed in a modified Arrhenius form:

$$k_{fj,rj} = k_0 T^n e^{-\frac{E_a}{RT}} \tag{1.7}$$

where k_0 is the pre-exponential factor, n the temperature exponent and E_a the activation energy. The rate constant for the forward reaction, k_{fj}, and for the reverse reaction, k_{rj}, are related through the equilibrium constant, K_{eq}, which can be found from the thermodynamic properties of the species [4]:

$$K_{eq} = \frac{k_{fj}}{k_{rj}} \quad . \tag{1.8}$$

Of course a single species may undergo not one, but several reactions. In this case the final expression for the chemical production rate for M reactions is given by:

$$R_i = W_i \frac{d[A_i]}{dt} = W_i \sum_{j=1}^{M} \left[k_{fj} r_{ij} \prod_{i=1}^{N} [A_i]^{r_{ij}} - k_{rj} p_{ij} \prod_{i=1}^{N} [B_i]^{p_{ij}} \right], \tag{1.9}$$

where W_i is the molecular weight of species A_i. A set of elementary reactions describing a combustion process from reactants to products constitutes a chemical mechanism. The GRI-Mech 3.0 chemical mechanism proposed by Smith et al [6] is widely used in the combustion field for describing methane oxidation including NO formation. The mechanism was developed under the sponsorship of the Gas Research Institute and consists of 325 elementary reactions and 53 chemical species [7]. The experimental data in this work was modeled using this chemical mechanism.

1.2 Mechanisms of nitric oxide formation

Nitric oxide (NO) is the primary nitrogen oxide emitted in combustion processes [8] and is a precursor for the formation of other nitrogen oxides (such as NO_2) [9]. In the combustion of fuels that do not contain nitrogen compounds, NO is formed from molecular nitrogen in air by breaking the triple bond between nitrogen atoms in N_2. There are four distinct routes responsible for the formation of NO in these fuels, which differ in the way in which the N_2 bond is broken, as illustrated in Figure 1.3:

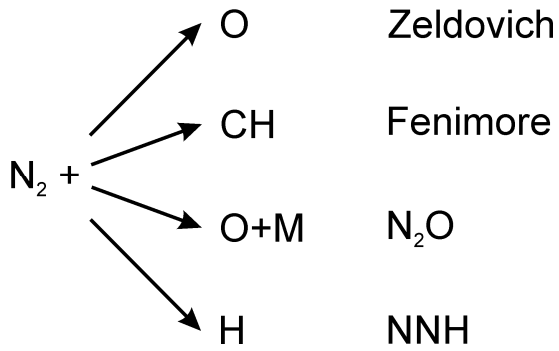

Figure 1. 3. Illustration of reactions leading to breaking the N_2 bond for forming NO under combustion conditions.

Some reactions can lead directly to NO, such as the Zeldovich mechanism, others shown in Figure 1.3 are first steps in a chain of reactions leading to NO. The important features of each reaction illustrated in Figure 1.3 will be discussed in this section.

1.2.1 Zeldovich or thermal mechanism

The thermal or Zeldovich mechanism, named after Y.B. Zeldovich who first postulated the mechanism in 1946 [10], consists of two principal reactions [3,9]:

$$O + N_2 \overset{k_{f1}}{\Leftrightarrow} NO + N \qquad k_{f1} = 1.8 \cdot 10^{14} \exp(-318 kJmol^{-1}/RT) \quad \text{(R 1.2)}$$

$$O_2 + N \overset{k_{f2}}{\Leftrightarrow} NO + O \qquad k_{f2} = 9.0 \cdot 10^{9} \exp(-27 kJmol^{-1}/RT) \quad \text{(R 1.3)}$$

The reaction between OH and N, which is important in fuel-rich flames where [OH]>>[O] is also considered as part of the Zeldovich mechanism [3,9]:

$$OH + N \overset{k_{f3}}{\Leftrightarrow} NO + H \qquad k_{f3} = 2.8 \cdot 10^{13} \qquad \text{(R1.4)}$$

The rate coefficients of these reactions haven been studied extensively and are well known (see [11]). Reaction (R 1.2) is considered to be the rate-determining step due to its relative high activation energy; this allows the reaction to proceed at considerable rate only at higher temperatures, typically above 1800 K. For this reason NO formed via the Zeldovich mechanism is referred to as "thermal NO".

Assuming that the initial concentration of NO is low, such that only forward reactions are considered, and that nitrogen atoms are in steady state, an expression can be derived for describing the overall rate of thermal NO formation:

$$\frac{d[NO]_{zeld}}{dt} = 2k_{f1}(T)[O][N_2], \qquad (1.10)$$

In most cases of air-fed combustion, the molecular nitrogen concentration does not vary substantially and the thermal NO formation rate depends only on temperature, through reaction rate k_{f1}, and the atomic oxygen concentration. To illustrate this temperature dependence, the thermal NO formation rate using Eq. (1.10) is calculated as function of flame temperature for three equivalence ratios while assuming equilibrium concentrations of O atoms and N_2 molecules. The results of these calculations are shown in Figure 1.4:

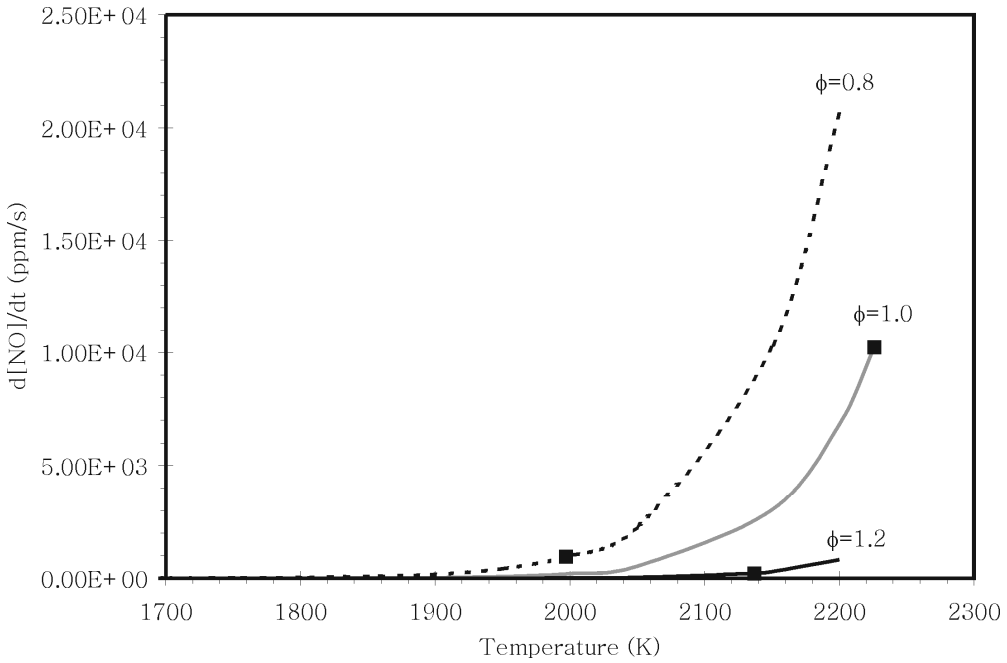

Figure 1. 4. Calculated thermal NO rate of production as function of flame temperature for premixed adiabatic methane/air flames at atmospheric pressure for ϕ=0.8, 1.0 and 1.2. Closes squares denote the adiabatic temperatures for the equivalence ratios assuming reactants at room temperature.

As can be seen from this Figure, the thermal NO formation rate shows significant acceleration at higher temperatures. Besides the temperature dependence, the calculations also show a strong dependence on the equivalence ratio: for fuel-rich conditions (ϕ=1.2) thermal NO formation is much slower in comparison to fuel-lean conditions (ϕ=0.8). In general, thermal NO formation is the dominant route to NO for fuel-lean and stoichiometric hydrocarbon flames [8]. The dependence on equivalence ratio reflects the difference in atomic oxygen concentration: for example, at a constant temperature of 1900 K, we observe an O atom concentration of 57.2 ppm for ϕ=0.8 and 0.24 ppm for ϕ=1.2. Under adiabatic conditions, the maximum thermal NO formation rate is achieved near stoichiometric conditions due to the simultaneous high adiabatic flame temperature and atomic oxygen concentration.

Based on equation (1.10), the actual amount of NO formed in a flame can be estimated. A typical flame length of ~10 cm and average burned gas velocity of 2 m/s result in a residence time of ~50 milliseconds. For this residence time the amount of thermal NO formed at stoichiometric conditions is about 500 ppm, which is much lower than the equilibrium value of ~1870

ppm. On the fuel-lean and fuel-rich sides of stoichiometric, the amount of NO formed decreases to 50 ppm (ϕ=0.8) and 10 ppm (ϕ=1.2) NO, respectively.

So far, an equilibrium concentration of O atoms was assumed: however, in the flame front the O-atom concentration can often significantly exceed the equilibrium value [9]. This so-called "superequilibrium concentration" is responsible for an acceleration of thermal NO formation in the flame front. While there is a contribution from superequilibrium O atoms to the Zeldovich NO formation under stoichiometric and fuel-lean condition [8], the results do not alter the trends shown in Figure 1.4.

Figure 1.5 shows a temperature and NO profile for a burner stabilized atmospheric pressure stoichiometric premixed methane/air flame, calculated using GRI-Mech 3.0 [6] and the CHEMKIN PREMIX code [5].

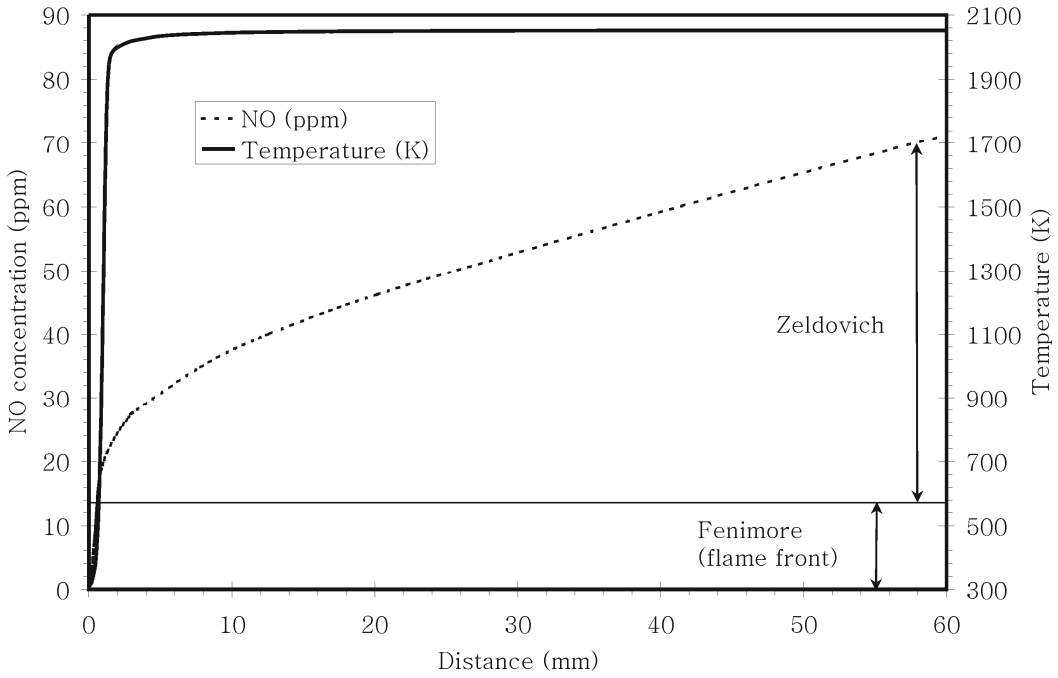

Figure 1.5. Calculated NO and temperature profile for an atmospheric pressure premixed methane-air flame at a mass flux of 0.025 g/cm^{2}s and ϕ=1.0. NO formation via Zeldovich and Fenimore mechanism (see § 1.2.2) are indicated.

Figure 1.5 shows that NO formed via the Zeldovich mechanism occurs primarily in the burned gas zone and that the NO concentration takes a long time to reach equilibrium, reflecting that thermal NO formation is rather slow at these temperatures.

Equation (1.10) shows that reducing the temperature and/or O atom concentration, for example by fuel-lean combustion [12-14], results in a reduction in thermal NO formation. Although this NO control strategy is used in many combustion processes, thermal NO formation is not the dominant NO formation route in fuel-rich flames, which we will discuss in the next section.

1.2.2 Fenimore mechanism

In 1971, Fenimore [15] suggested an additional NO formation mechanism based on the observation that NO profiles measured in atmospheric-pressure hydrocarbon flames, when extrapolated to the burner surface, yielded non-zero NO concentrations in the flame front, especially for fuel-rich conditions. Fenimore concluded that NO was formed near the burner surface, in the flame front, and called this "prompt NO" (see also Figure 1.5). Based on these observations, Fenimore suggested that rate-determining step for this fast NO formation is due to the reaction of nitrogen with hydrocarbon radicals, such as:

$$CH + N_2 \overset{k_{f4}}{\Leftrightarrow} HCN + N \qquad k_{f4}(T) = 3.12\times10^{9} T^{0.88} \exp(-84 kJmol^{-1}/RT), \text{ (R 1.5)}$$

where the rate coefficient is taken from [6]. The hydrogen cyanide (HCN) and nitrogen atom (N) produced in reaction (R 1.5), reacts subsequently to NO through a series of reactions [9]. Suppose we assume that all N and HCN formed via reaction (R 1.5) rapidly react to NO and neglect the reverse reaction; then the amount of NO formed via the Fenimore mechanism can be calculated by integrating equation (1.9), similar to that done in [16,17]:

$$X_{NO,Fen} = \frac{2\overline{W}}{\rho v}\int k_{f4}[T(x)]\cdot CH(x)\cdot N_2(x)\left(\frac{P}{RT(x)}\right)^2 \cdot dx, \qquad (1.11)$$

where $X_{NO,Fen}$ is the mole fraction Fenimore NO, $CH(x)$, $N_2(x)$, $T(x)$, $v(x)$ and $\overline{W}(x)$ the local CH mole fraction, nitrogen mole fraction, temperature, gas velocity and local mean molecular weight, respectively, and P the pressure. In a similar way the amount of thermal NO can be calculated:

$$X_{NO,Zeld} = \frac{2\overline{W}}{\rho v}\int k_{f1}[T(x)]\cdot O(x)\cdot N_2(x)\left(\frac{P}{RT(x)}\right)^2 \cdot dx, \qquad (1.12)$$

where $X_{NO,Zeld}$ is now the mole fraction Zeldovich NO and O(x) is the local oxygen atom concentration.

Figure 1.6 shows the results of calculating the Fenimore and Zeldovich NO mole fractions as function of the equivalence ratio, using equations (1.11 and 1.12) and predictions from the CHEMKIN calculations for atmospheric-pressure methane/air flames.

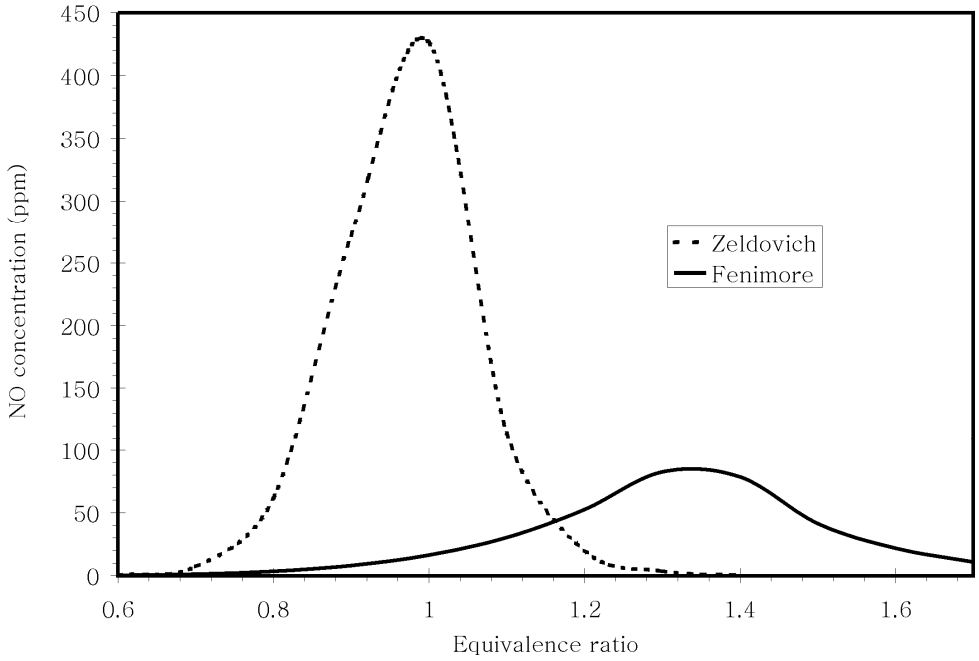

Figure 1. 6. Calculated Zeldovich and Fenimore NO mole fractions as function of the equivalence ratio. Integration was performed up to 10 cm above the burner surface.

As shown in Figure 1.6, the Fenimore NO is the dominant route for NO production in fuel-rich (ϕ greater than roughly 1.2) methane/air flames. The maximum Fenimore NO concentration is observed near ϕ=1.4.

The CH radicals, important for Fenimore NO formation, are formed via the route [9]: $CH_4 \rightarrow CH_3 \rightarrow CH_2 \rightarrow CH$. For $1.1 < \phi \leq 1.4$, the following reaction is primarily responsible for the creation of CH radicals [18]:

$$CH_2 + H \quad \Leftrightarrow \quad CH + H_2. \qquad (R\ 1.6)$$

Once the CH radicals thus formed react with nitrogen according to reaction (R 1.5), the HCN and N produced react rapidly to form NO according to the following reactions [9]:

$$HCN + O \Leftrightarrow NCO + H \quad \text{(R 1.7)}$$
$$NCO + H \Leftrightarrow NH + CO \quad \text{(R 1.8)}$$
$$NH + H \Leftrightarrow N + H_2 \quad \text{(R 1.9)}$$
$$OH + N \Leftrightarrow NO + H \quad \text{(R 1.4)}$$

For ϕ>1.4, the decrease in O, OH and H radical concentrations becomes important [see reaction (R1.6)], causing a decrease in CH concentration and consequently a decrease in the resultant concentration of Fenimore NO.

Equation (1.11) shows that besides the CH concentration, the temperature is another important parameter for Fenimore NO formation. The activation energy of reaction (R 1.5) is considerably lower than the activation energy of reaction (R 1.2), allowing prompt NO formation to take place at temperatures as low as 1000 K.

Since Fenimore first proposed his mechanism, much progress has been made in understanding the mechanism, but despite this advance there are still significant uncertainties. For example, detailed information on the rate constant of reaction (R 1.5) is scarcely available in the literature. The reaction rate constant used in GRI-Mech 3.0 [6] was determined by fitting high temperature shock tube data (2300<T<3800 K) [19,20] and optimizing for the peak CH concentration measured in a low-pressure flame [21] (T<1730 K). The relatively large scatter in the data in the high temperature range increases the uncertainty in the rate constant. Moreover, for an important regime for combustion between 1730 and 2300 K there are no direct measurements of rate constant for reaction (R 1.5) and experiments in this area are needed to validate or improve its value. A consequence of this gap in the temperature range is that the predictions of NO formed via the Fenimore mechanism are uncertain.

Another issue in the Fenimore mechanism is the uncertainty in which products are formed from reaction (R 1.5). Moskaleva et al. [22] suggested that since reaction (R 1.5) is spin-forbidden other products should be preferred, and

based on theoretical considerations proposed the following reaction instead of (R 1.5):

$$CH + N_2 \Leftrightarrow NCN + H \qquad \text{(R 1.10)}$$

Using reaction (R 1.10) instead of reaction (R 1.5) as rate-determining step in Fenimore NO formation can be one of the reasons for the observed differences between measurements and model predictions for flames in which the Fenimore mechanism is dominant [13,14,23]. Smith [24] detected NCN in low-pressure methane/air and methane/NO flames: the presence of NCN in these flames suggests its role as an intermediate in nitrogen chemistry. However, since little is known about the mechanism for conversion of NCN to NO, it is difficult to assess whether (R 1.10) or (R 1.5) is the rate-determining step.

There are not only uncertainties in the products of reaction (R 1.5), but also in the reactions involved in CH radical formation. As discussed above, CH is primarily formed via reaction (R 1.6). The two most important consumption reactions for CH are:

$$CH + H_2O \Leftrightarrow CH_2O + H \qquad \text{(R 1.11)}$$

$$CH + O_2 \Leftrightarrow HCO + O. \qquad \text{(R 1.12)}$$

Especially reaction (R 1.11) has a large uncertainty [11] in the reaction rate, which affects the CH chemistry and therefore also the NO formation.

Apart from uncertainties in reaction rates for CH chemistry, another problem is the measurement of CH, which exists only in the flame front. Figure 1.7 shows calculated CH profiles using GRI-Mech 3.0 for flames at 100 and 761 Torr:

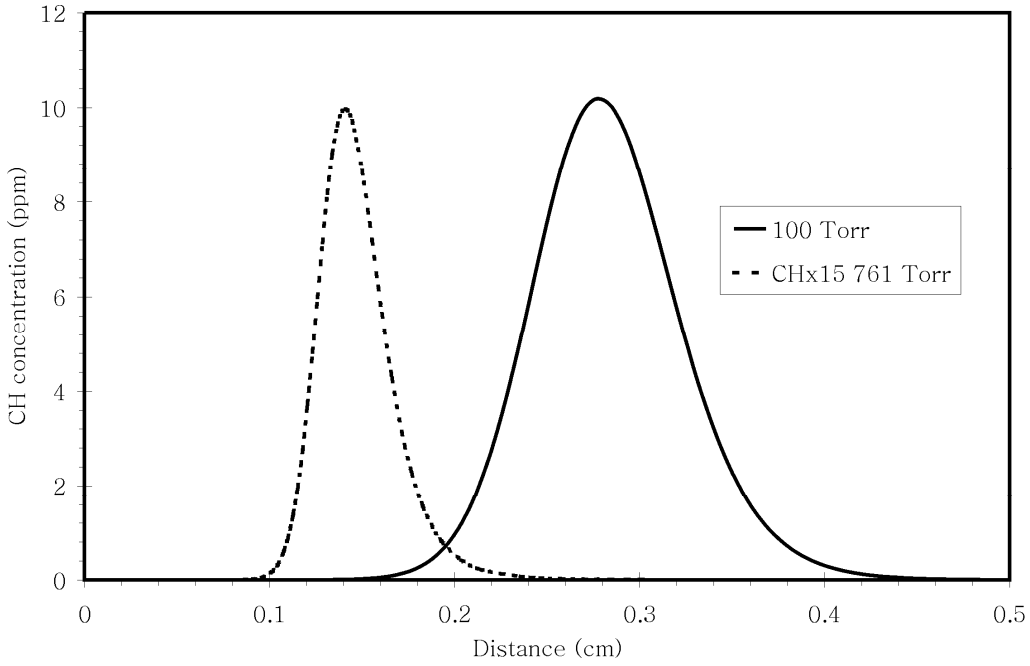

Figure 1. 7 Calculated CH profiles for 100 and 761 Torr. CHEMKIN calculations are performed for ρv=0.00721 g/cm^{2}s premixed ϕ=1.2 methane/air flames.

At atmospheric pressure the CH profile is very narrow and CH concentrations are very low, which makes measurements on CH very difficult [25]. However, when lowering the pressure the flame front broadens, which facilitates performing measurements of CH, as well as of other important flame parameters which have steep gradients, such as temperature and other species present in the flame front. Thus, at reduced pressures the profiles of CH and NO can be relatively easily resolved, which helps us to gain insight in the complex Fenimore mechanism.

1.2.3 Other NO formation mechanisms

N_2O mechanism

In the nitrous oxide (N_2O) mechanism [9], NO is formed through N_2O intermediate species that is produced according to the following reaction:

$$N_2 + O + M \Leftrightarrow N_2O + M \qquad \text{(R 1.13)}$$

The N_2O may react subsequently with O or H atoms to form NO:

$$N_2O + O \Leftrightarrow NO + NO \quad \text{(R 1.14)}$$

$$N_2O + H \Leftrightarrow NO + NH \quad \text{(R 1.15)}$$

This reaction is primarily occurs under lean conditions, at low temperatures and elevated pressures [8]. With the exception of lean premixed combustion in gas turbine engines [26], this mechanism has only a minor contribution to the total formation of NO in comparison with the Zeldovich and Fenimore mechanisms.

NNH mechanism

This route for forming NO was suggested by Bozzelli and Dean [27], where NO was formed by oxidation of NNH radicals:

$$H + N_2 \Leftrightarrow NNH \quad \text{(R 1.16)}$$

$$NNH + O \Leftrightarrow NO + NH \quad \text{(R 1.17)}$$

The NNH mechanism was suggested to be the dominant source of NO production in low temperature fuel-rich premixed hydrogen air flames, where the contribution from Zeldovich is suppressed [28,29].

1.3 Nitric oxide emission reduction by flue-gas recirculation and upstream heat-loss in fuel-rich premixed flames

As mentioned before, combustion modifications for controlling NO emissions from combustion equipment fired with natural gas are almost always aimed at suppressing the contribution from Zeldovich mechanism by reducing the flame temperature and/or lowering oxygen concentration, according to equation (1.12). In this thesis we will focus on two temperature reduction methods: flue-gas recirculation (FGR, dilution of fuel-air mixture with N_2+CO_2) and upstream heat-loss (burner stabilization, operating principle of radiant burners).

1.3.1 Upstream heat-loss

Figure 1.8 shows a schematic drawing of the principle of upstream heat loss:

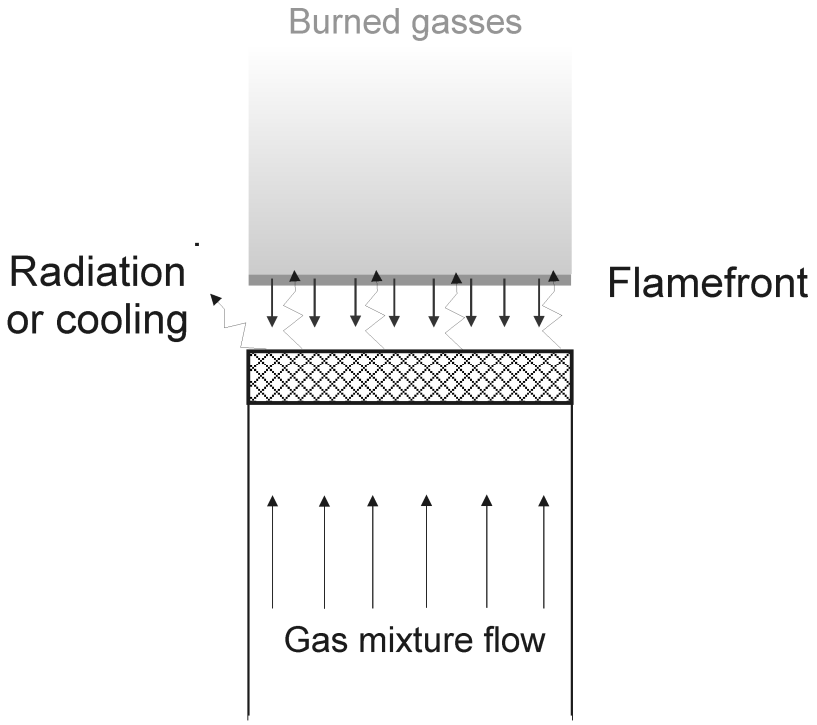

Figure 1. 8. Operating principle of upstream heat loss

As mentioned above, when the cold gas velocity is lower than the free flame burning velocity, heat from the flame is transferred to the burner surface, which is transferred to the surroundings either as radiation or into the cooling water in water-cooled burners such as the McKenna Products burner. Except for the difference in heat transfer, flames stabilized on both burners have identical characteristics at the same exit velocity [14]: heat lost to the surroundings lowers the flame temperature by the same amount in comparison with adiabatic temperature. To illustrate this principle, calculations have been performed for an atmospheric pressure ϕ=1.3 premixed methane/air flame for different cold gas exit flows. Figure 1.9 shows the flame temperature as function of cold gas velocity.

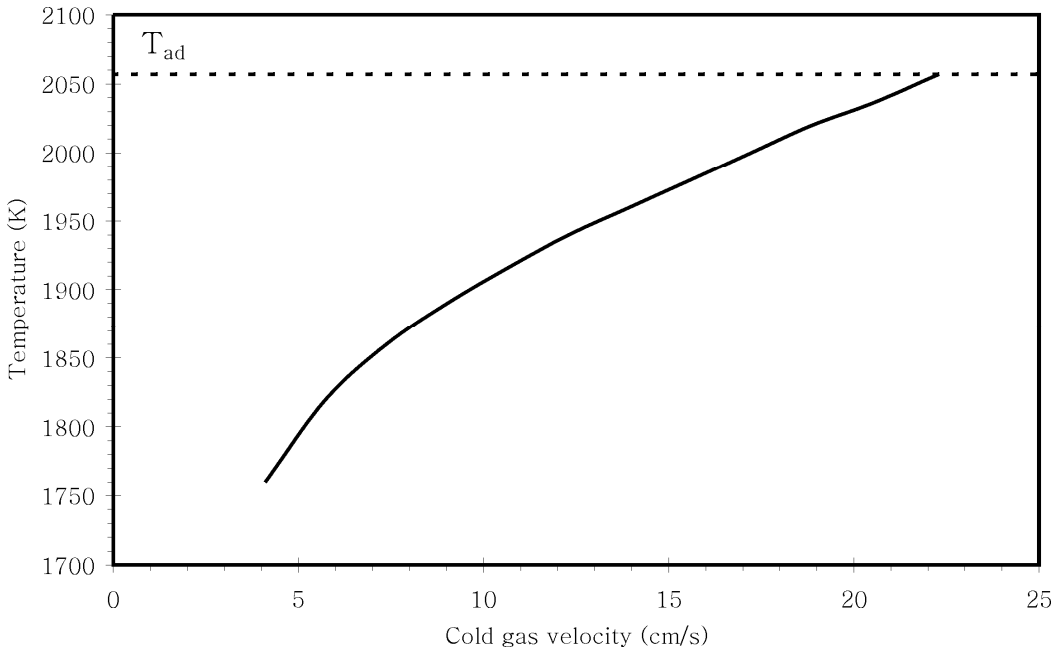

Figure 1. 9. Calculated flame temperatures as function of cold gas velocity. CHEMKIN calculations are performed atmospheric pressure ϕ=1.3 premixed methane/air flame.

As can be seen in the Figures, lowering the cold gas velocity in this flame by a factor of 4 decreases the flame temperature by ~250 K. However, we cannot infinitely decrease the flow rate in order to achieve lower temperatures: at a certain point the flame temperature is too low for a flame to exist, and the flame extinguishes. This minimum cold gas velocity and corresponding temperature form a fundamental limit for this method of NO_x control.

While the effects of decreasing temperature on Zeldovich NO formation is well understood [12-14], the quantitative relation between temperature decrease and changes in NO formation via Fenimore mechanism remains unclear, due to the uncertainties in this mechanism, as discussed above.

Mokhov and Levinksy [13,14] measured the temperature and NO profiles in atmospheric pressure premixed natural gas/air and methane/air flames, where the flame temperature was changed by upstream heat-loss. The 'expected' NO reduction was observed for fuel-lean flames, where the Zeldovich mechanism is dominant. In fuel-rich flames, however, where the NO concentration is expected to be less sensitive to flame temperature changes because of the lower activation energy than for the Zeldovich mechanism, the experiments show a significant decrease in NO concentration for fuel-rich conditions with temperature: over a range of 100 K the NO concentration

decreases by a factor of 2 [13]. The temperature range of these experiments was extended by Sepman, et al. [30] using preheated reactants, in which a factor of 2 decrease in Fenimore NO was observed over 400 K at ϕ=1.3. Interestingly, a very sharp change in Fenimore NO was observed at ϕ=1.5; by a factor of 9 over a range of 100 K.

The experimental results were compared with predictions of numerical models; the models predicted the response for fuel-lean and stoichiometric flames well [13,30], but predicted the absolute values at ϕ=1.3 substantially more poorly [20]. Interesting as well was the good prediction of the results at ϕ=1.5 [30]. These results show that more insight in the behavior of these models is needed, but also indicates the possibility of 'alternative' low-NO_x strategies based on fuel-rich combustion. To achieve this, experimental investigations of Fenimore NO formation as a function of temperature are needed.

1.3.2 Flue-gas recirculation

Flue-gas recirculation (FGR) is a well-known NO_x emission control strategy often used in industrial burners, such as large-scale utility boilers, where NO reductions of 70 percent can be achieved [8]. In FGR, a portion of the flue gases produced by the combustion process is recycled back to the burner by mixing with fuel or oxidizer [2]. In this work we study 'dry' FGR, which means that water is removed prior to mixing with fuel or oxidizer, as is often done in practice to avoid condensation of water and corrosion in the pipelines recirculating the flue gases. The cold 'inert' flue gases (such as N_2 and CO_2) are heated up by the flame, resulting in a lower flame temperature and consequently lower NO emissions. To a lesser extent, dilution with flue gases lowers the initial oxygen levels in the flame, which in turn lowers thermal NO formation (see also 1.12 and § 1.2.1).

Increasing the amount of flue gas recirculation, results in a decrease in NO formation. However, we cannot increase this amount indefinitely: excessive flue-gas produces instable flames, resulting in an unwanted increase in CO emissions and ultimately in blow-off of the flames.

Mokhov and Levinsky [14] studied the effectiveness of upstream heat loss and FGR as NO_x control strategies, and for stoichiometric flames observed the

same reduction in NO mole fraction, independent of the NO control strategy. However, for flames at ϕ=1.3 the measured NO mole fractions using FGR were significantly higher in comparison to those measured for burner stabilization.

1.4 Studies of NO formation in low-pressure flames

To determine how FGR and upstream heat loss influence NO formation in fuel-rich methane-air flames, it is necessary to measure the key intermediates involved in the Fenimore mechanism. As discussed above, the CH radical plays a key role in this process, but is difficult to measure at atmospheric pressure. Only a few CH-radical measurements have been performed at atmospheric pressure [25,31]; the measurements were performed for development of laser diagnostics where, in case of Ref [25], results were compared with calculations without drawing conclusions regarding the mechanism.

Almost all quantitative measurements of CH concentration have been performed at reduced pressure. For example, Berg et al. [21] measured temperature and absolute CH profiles in premixed low-pressure methane/oxygen/nitrogen flames for different equivalence ratios (ϕ = 0.81, 1.07 and 1.28 with varying N_2/O_2 ratios) and compared experimental results with predictions using GRI Mech 3.0. Predictions showed the expected good agreement with the measured CH profile for the flame used as a target in optimizing the mechanism (ϕ=1.07), but discrepancies were found both for leaner and richer flames in terms of maximum CH concentration and width of the CH profile. Failing to predict the position of the CH profile results in large uncertainties in prediction of Fenimore NO [1,16].

To date, only a few studies have been devoted to Fenimore NO formation in fuel-rich, low-pressure, methane-air flames [1,16,17,21]. However, these studies are restricted to ϕ<1.3, and none of them consider the effects of FGR and upstream heat loss. In this thesis, we examine the effect of these two NO_x control strategies on NO formation in fuel-rich methane-air flames at low-pressure. Towards this end, the profiles of temperature and the mole fractions of CH, OH and NO are measured for ϕ=1.3-1.5. Since this parameter variation represents a substantial extension to the previous studies; the results are also used to test the predictions of GRI-Mech 3.0.

Bibliography

1. Heard, D. E., Jeffries, J. B., Smith, G. P., and Crosley, D. R., "Lif Measurements in Methane Air Flames of Radicals Important in Prompt-No Formation", *Combust.Flame* **88**, 137-148 (1992)

2. Turns, Stephen R., *An introduction to combustion : concepts and applications*, (McGraw-Hill, New York, 1999)

3. Warnatz, Jürgen, Maas, Ulrich, and Dibble, Robert W., *Combustion : physical and chemical fundamentals, modelling and simulation, experiments, pollutant formation*, (Springer, Berlin, 1999)

4. Fristrom, R. M. and Westenberg, A. A., *Flame structure*, (McGraw-Hill, New York, 1965)

5. Kee, R. J., Rupley, F. M., and Miller, J. A., "CHEMKIN II: A Fortran Chemical Kinetics Package for the Analysis of Gas-Phase Chemical Kinetics", Report No.SAND89-8009, Sandia National Laboratories ,1989

6. Smith, G. P., Golden, D. M., Frenklach, M., Moriarty, N. W., Eiteneer, B., Goldenberg, W., Bowman, C. T., Hanson, R., Gardiner, W. C, Lissianski, V., and Qin, Z., http://www.me.berkeley.edu/gri_mech/.

7. Simme, J. M., "Detailed Chemical Kinetic Model for the Combustion of Hydrocarbon Fuels", *Prog.Energy Combust.Sci.* **29**, 599-634 (2003)

8. Bowman, C. T., "*Control of Combustion-Generated Nitrogen Oxide Emissions: Technology Driven by Regulation*", 24th Symp. (Int.) Combust., 859-878 (1992)

9. Miller, J. A. and Bowman, C. T., "Mechanism and Modeling of Nitrogen Chemistry in Combustion", *Prog.Energy Combust.Sci.* **15**, 287-338 (1989)

10. Zeldovich, Y. B., "The Oxidation of Nitrogen in Combustion and Explosions", *Acta Physicochim.* **21**, 577-1946)

11. Baulch, D. L., Cobos, C. J., Cox, R. A., Frank, P., Hayman, G., Just, T., Kerr, J. A., Murrells, T., Pilling, M. J., Troe, J., Walker, R. W., and Warnatz, J., "Summary Table of Evaluated Kinetic Data for Combustion Modeling - Supplement-1", *Combust.Flame* **98**, 59-79 (1994)

12. Bouma, P. H. and De Goey, L. P. H., "Premixed Combustion on Ceramic Foam Burners", *Combust.Flame* **119**, 133-143 (1999)

13. Mokhov, A. V. and Levinsky, H. B., "*A LIF and CARS Study of the Effects of Upstream Heat Loss on NO Formation From Laminar Premixed Burner-Stabilized Natural-Gas/Air Flames*", 26th Symp. (Int.) Combust., 2147-2154 (1996)

14. Mokhov, A. V. and Levinsky, H. B., "*A LIF and CARS Investigation of Upstream Heat Loss and Flue-Gas Recirculation As NOx Control Strategies for Laminar, Premixed Natural-Gas/Air Flames*", 28th Symp. (Int.) Combust., 2467-2474 (2000)

15. Fenimore, C. P., "*Formation of Nitric Oxide in Premixed Hydrocarbon Flames*", 13th Symp. (Int.) Combust., 373-379 (1971)

16. Berg, P. A., Smith, G. P., Jeffries, J. B., and Crosley, D. R., "*Nitric Oxide Formation and Reburn in Low-Pressure Methane Flames*", 27th Symp. (Int.) Combust., 1377-1383 (1998)

17. Pillier, L., El Bakali, A., Mercier, X., Rida, A., Pauwels, J. F., and Desgroux, P., "*Influence of C-2 and C-3 Compounds of Natural Gas on NO Formation: an Experimental Study Based on LIF/CRDS Coupling*", 30th Symp. (Int.) Combust., 1183-1191 (2005)

18. Gersen, S.,*Numerieke simulatie van NO vorming in een-dimensionale voorgemengde methaan/lucht vlammen ,Rijksuniversiteit Groningen, (2001)*

19. Miller, J. A. and Walch, S. P., "Prompt NO: Theoretical Prediction of the High-Temperature Rate Coefficient for CH+N2->HCN+N", *Int.J.Chem.Kinet.* **29**, 253-259 (1997)

20. Rodgers, A. S. and Smith, G. P., "Pressure and Temperature Dependence of the Reactions of CH With N2", *Chem.Phys.Let.* **253**, 313-321 (1996)

21. Berg, P. A., Hill, D. A., Noble, A. R., Smith, G. P., Jeffries, J. B., and Crosley, D. R., "Absolute CH Concentration Measurements in Low-Pressure Methane Flames: Comparisons With Model Results", *Combust.Flame* **121**, 223-235 (2000)

22. Moskaleva, L. V. and Lin, M. C., "*The Spin-Conserved Reaction CH+N2 -> H+NCN: A Major Pathway to Prompt NO Studied by Quantum /Statistical Theory Calculations and Kinetic Modeling of Rate Constant*", 28th Symp. (Int.) Combust., 2393-2401 (2000)

23. Gasnot, L., Desgroux, P., Pauwels, J. F., and Sochet, L. R., "Detailed Analysis of Low-Pressure Premixed Flames of CH4+O2+N2: A Study of Prompt-NO", *Combust.Flame* **117**, 291-306 (1999)

24. Smith, G. P., "Evidence of NCN As a Flame Intermediate for Prompt NO", *Chem.Phys.Let.* **367**, 541-548 (2003)

25. Evertsen, R., Van Oijen, J. A., Hermanns, R. T. E., De Goey, L. P. H., and Ter Meulen, J. J., "Measurements of Absolute Concentrations of CH in a Premixed Atmospheric Flat Flame by Cavity Ring-Down Spectroscopy", *Combust.Flame* **132**, 34-42 (2003)

26. Correa, S. M., "A Review of Nox Formation Under Gas-Turbine Combustion Conditions", *Combust.Sci.Technol.* **87**, 329-362 (1993)

27. Bozzelli, J. W. and Dean, A. M., "*O+NNH - A Possible New Route for NOx Formation in Flames*", 27th Int. J. Chem. Kinet., 1097-1109 (1995)

28. Hayhurst, A. N. and Hutchinson, E. M., "Evidence for a New Way of Producing NO Via NNH in Fuel-Rich Flames at Atmospheric Pressure", *Combust.Flame* **114**, 274-279 (1998)

29. Harrington, J. E., Smith, G. P., Berg, P. A., Noble, A. R., Jeffries, J. B., and Crosley, D. R., "*Evidence for a New NO Production Mechanism in Flames*", 26th Symp. (Int.) Combust., 2133-2138 (1996)

30. Sepman, A. V, Mokhov, A. V., and Levinsky, H. B., "A Laser-Induced Fluorescence and Coherent Anti-Stokes Raman Scattering Study of NO Formation in Preheated, Laminar, Rich Premixed, Methane/Air Flames", *Symp.(Int.) Combust.* **29**, 2187-2194 (2002)

31. Mercier, X., Jamette, P., Pauwels, J. F., and Desgroux, P., "Absolute CH Concentration Measurements by Cavity Ring-Down Spectroscopy in an Atmospheric Diffusion Flame", *Chem.Phys.Let.* **305**, 334-342 (1999)